ORIGINAL PAPER

An aptamer based fluorometric assay for amyloid-β oligomers using a metal-organic framework of type Ru@MIL-101(Al) and enzyme-assisted recycling

Hong-Xia Ren[1] · Yang-Bao Miao[2] · Yuandong Zhang[3]

Abstract

Amyloid-beta (Aβ) oligomers causing neuron damage are regarded as potential therapeutic targets and diagnostic markers for Alzheimer's disease (AD). A homogeneous turn-on fluorometric aptasensor is described for Aβ oligomers. It is highly selective and non-invasive and based on (a) the use of a luminescent metal-organic framework carrying aptamer-modified AuNPs (L-MOF/Apt-Au) as tracking agent, and (b) enzyme-assisted target recycling signal amplification. The tracking agent does not emit fluoresce by fluorescence resonance energy transfer (FRET) between the luminescent MOF as donor and Apt-Au as the acceptor under the excitation wavelength of 466 nm. When Aβ oligomers are added to the tracking agent solution, the Apt-Au on tracking agent can preferentially bind with Aβ oligomers and then be released. This turns the "off" signal of the luminescent MOF tracer to the "on" state. The enzyme (Rec Jf exonuclease) added into the supernatant further improves sensitivity due to enzyme-assisted target-recycling signal amplification. The assay has an excellent linear response to Aβ oligomers from 1.0 pM to 10 nM, with a detection limit of 0.3 pM. This homogeneous turn-on fluorometric method is expected to have potential and applications in clinical diagnosis.

Keywords Luminescent metal-organic framework · Enzyme assisted target recycling · Tracking agent · Homogeneous assay · Turn-on fluorometry

Introduction

Early and accurate diagnosis of Alzheimer's disease (AD) has a major impact on the progress of research on dementia [1–3]. The Aβ oligomers are potent diagnostic markers and thera-

✉ Hong-Xia Ren
renhongxiahappy@126.com

1 School of Chemistry and Chemical Engineering, Zunyi Normal College, Guizhou 563006, China

2 Department of Chemical Engineering and Frontier Research Center on Fundamental and Applied Sciences of Matters, National Tsing Hua University, Hsinchu 30013, Taiwan

3 School of Pharmacy, Zunyi Medical University, Guizhou 563000, China

peutic targets for AD [4, 5]. Developing a non-invasion and precise method for the detection of Aβ oligomers for the early diagnosis of AD and the screening of drugs for AD treatment is significantly important [6]. In particular, the detection of Aβ oligomers with specific selectivity is a challenge due to the complex environment of Aβ oligomers in plasma [7].

Among the various methods for Aβ oligomers determination, antibody or single-chain antibody fragments are one of the most common tools [8]. Based on antibody recognition, enzyme-linked immunosorbent assay (ELISA) type assays are frequently applied for determination of Aβ oligomers in patient fluids. Compared with antibodies, Aptamers which are DNA or RNA sequences own the advantages of easy preparation, chemical stability and design versatility [9, 10]. Fortunately, aptamers with high affinity and specifity for oligomeric amyloid proteins were selected (dissociation constants (Kd) spanning from 29 to 48 nM) [11]. Aptamer was the recognition element of aptamer sensors, which combine the recognition process with the versatile DNA molecular tools [12]. For the trace level determination, the traditional aptamer

sensors is difficult, while the nuclease (endonuclease and exonuclease)-assisted target recycle can effectively increase the signal with especially noticeable outcome [13, 14]. The exonuclease has become more and more popular for DNA amplification determination, which need no specific recognition sequence of nucleic acid [15]. For instance, Rec Jf exonuclease can decompose single-strand DNA along the direction of 5′ to 3′ and release target again for probe reaction [16, 17]. The exonuclease-assisted target recycling is very straight and requires no further immobilization step, which has been diffusely used for signal amplification [16].

Luminescent metal-organic frameworks (L-MOF) have experienced explosive growth for their specific features, such as flexibility, structural diversity, high porosity, tailorability, large surface area and extraordinary adsorption affinities [18–20]. Most of the reports on fluorometric assays via L-MOFs are susceptible to environmental interference, which limited the application of L-MOF [21, 22]. Developing a sensitive and homogeneous fluorescence "turn-on" determination strategy is necessary. To fulfill the requirement of homogeneous and "turn-on" fluorescence amplification strategy, luminescence metal-organic frameworks (L-MOFs) of nanoporous material have been associated with exonuclease-assisted target recycling signal amplification techniques. L-MOF of nanoporous material display a wide range of luminescent behaviors resulted from the multifaceted nature of their structure and can effectively protect macromolecules from being destroyed by enzyme via nanoporous, such as proteins, DNA and RNA [17, 23]. Therefore, the L-MOFs adsorbing DNA aptamer was designed.

The novel homogeneous "turn-on" fluorescent aptasensor for Aβ oligomers determination based on L-MOFs nanocomposites as tracking agent with exonuclease-assisted target recycling is illustrated in Scheme 1. The tracking agent was obtained by electrostatic adsorption or π stacking between aptamer labeled nano-gold (Apt-Au) and Ru,Al-MOF [24]. This probe is in "turn-off" state without fluoresce emitting because the signal from Ru,Al-MOF's as donor with excellent fluorescence properties under excitation light is quenched by the Apt-Au as acceptor. Adding Aβ oligomers into the composite probe solution, the Apt-Au on composite probe can preferentially bound with Aβ oligomers and then be released from the composite probe turning the "off" signal of luminescence MOF tracer to "on" state. The enzyme (Rec Jf exonuclease) added into the supernatant can generate high sensitivity resulted from enzyme-assisted target recycling signal amplification. This strategy can distinguish of trace levels of Aβ oligomers by fluorescence spectrophotometer based on L-
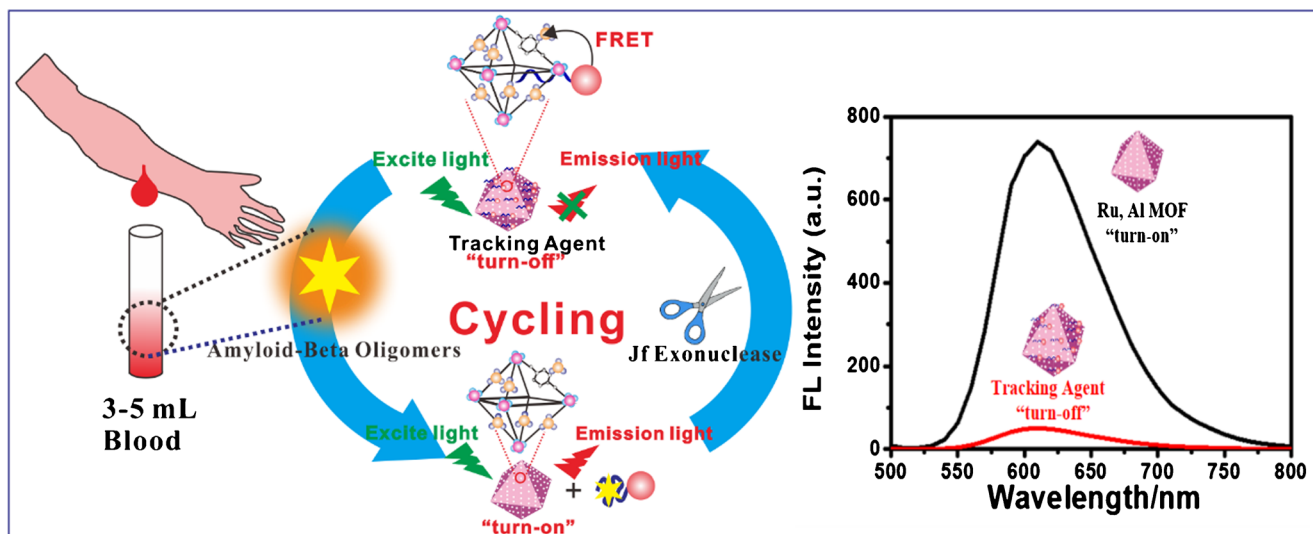
MOF nanocomposites as tracking agent with enzyme-assisted target recycling.

Experimental section

Reagents and chemicals The oligonucleotides was synthesized by Sangon Biotechnology Co. Ltd. (https://www.sangon.com/, Shanghai, China) as the following sequences: The 27-mer high affinity of aptamers toward Aβ oligomers 3′NH$_2$-(CH$_2$)$_6$-GCTGC CTGTG GTGTT GGGGC GGGTG CG [11]; AlCl$_3$, Tris(2,2′-bipyridine-n,n′)dichloride, hexahydrate, 1,4-dicarboxybenzene, Chloroauric Acid were from Sinopharm Chemical Reagent Co., Ltd. ((https://www.sinoreagent.com/, Shanghai, China). The Aβ oligomers ELISA Kit and Rec Jf exonuclease, Cholesterol, Hemoglobin, Plasma protein, Lipoprotein, Albumin, Globulinds was purchased from Takara Biotechnology Co. Ltd. (http://www.takarabiomed.com.cn/, Dalian, China). Phosphate buffer saline (PBS, pH 7.4, 0.1 M KH$_2$PO$_4$-K$_2$HPO$_4$, 0.1 M KCl) was used as washing and binding buffer. The blocking buffer solution was PBS (pH 7.4) containing 3% (w/v) BSA. Tris-HCl buffer (0.1 M) containing 0.1 M NaCl and 5 mM MgCl$_2$ (pH 7.4) was employed for preparation of DNA stock solutions. All other reagents were analytical grade and were used without further purification. Double-distilled water was used throughout the study.

Apparatus The transmission electron microscopic (TEM) image was from a H600 transmission electron microscope (Hitachi, Japan). The UV-vis spectra were recorded by a UV-1800 spectrophotometer (Shimazu Co., Japan). The fluorescence spectrophotometer recorded by a FL-4600 fluorescence spectrophotometer (Shimazu Co., Japan). Dynamic Light Scattering was carried out by the Malvern zetasizer Nano ZS90, Malvern instruments Ltd., UK with a 50 mV laser.

The synthesis of tracking agent The Ru, Al MOF was obtained according to the literature with small-scale modification [25]. Briefly, 58.17 mg Al$_2$(SO$_4$)$_3$ (0.17 mmol), 29 mg benzene 1,4 dicarboxylate (0.17 mmol), 394 μL glacial acetic acid (6.8 mmol) and 40 mg Ru(II)(2,2′-bipyridine)$_3$Cl$_2$ in 15 mL of dimethyl formamide and 15 mL deionized (DI) water were heated at 120 °C for 24 h producing an orange crystalline powder and then was cooled to room temperature. The precipitation was isolated by centrifugation. To remove excess reactants, the powder was washed with ethanol and DMF. Then the powder was washed extensively first with DMF and then ethanol (four wash-centrifuge cycles each). The octahedron particles were dried in a vacuum oven at 35 °C.

Scheme 1 Schematic of the fluorometric method for determination of Aβ oligomers based on L-MOF nanocomposites as tracking agent with exonuclease-assisted target recycling

By the SEM images of octahedron of MOFs after 6 months, the product in the form of solid powder was stable in organic solvents and water.

The immobilization of aptamer-Au NPs onto the Ru, Al MOF was carried out according to the procedure as previously reported [26, 27]. In brief, 100 μL of amino functionalized aptamer (100 mg·mL^{-1}) and 5 mL Au NPs (100 mg·mL^{-1}) solution were reacted for 4 h at room temperature, washed with washing buffer and collected by 12,000 rpm centrifugation for 10 min. Then, the Ru, Al MOF were incubated at 4 °C with 1.0 mL PBS containing aptamer-Au NPs (100 μL, 100 mg·mL^{-1}) for 12 h.
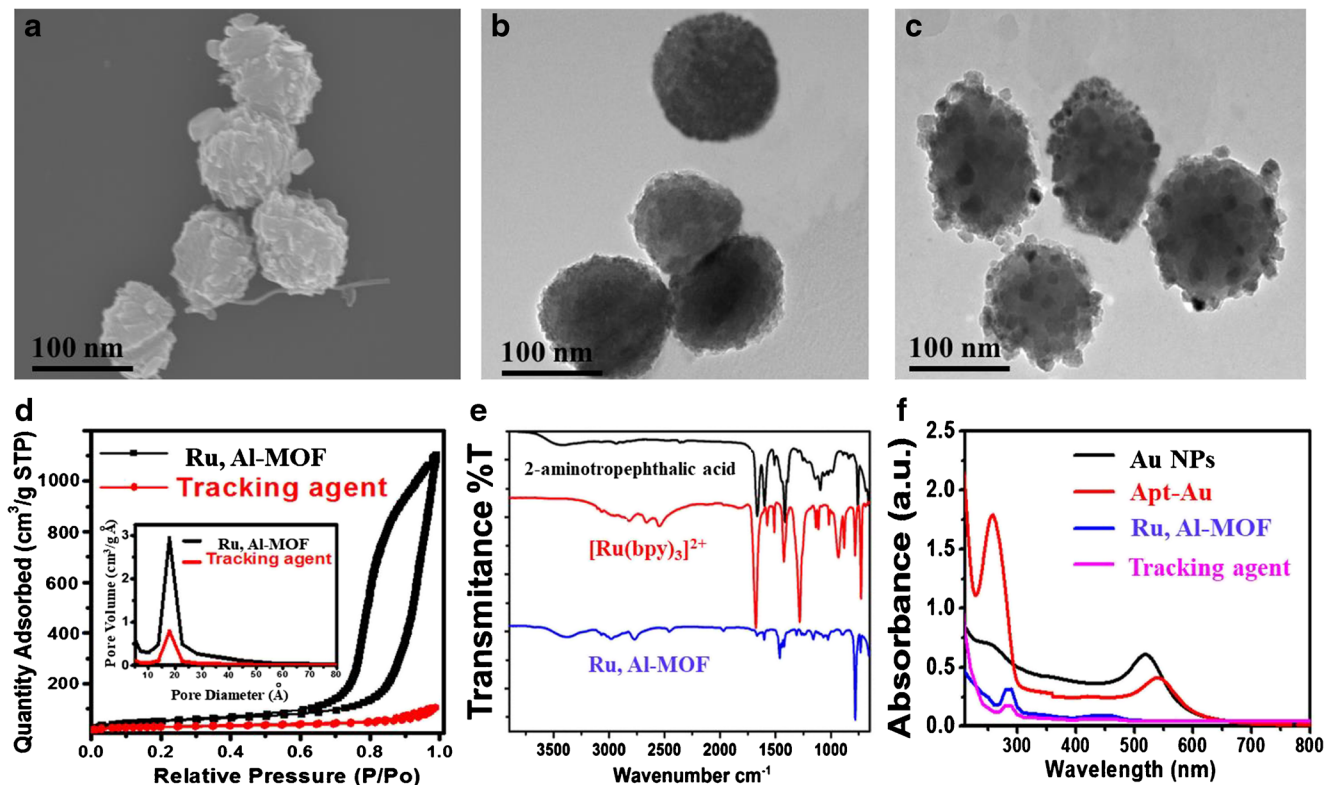

Fig. 1 SEM images of Ru,Al-MOF nanospheres (**a**), TEM images of Ru,Al-MOF nanospheres (**b**), TEM images of tracking agent (**c**), BET surface area for meso Ru,Al-MOF nanospheres (inset: pore diameter of Ru,Al-MOF nanospheres and tracking agent) (**d**), The FTIR spectra of 2-aminotropephthalic acid (black curve), [Ru(bpy)$_3$]$^{2+}$ (red curve), Ru,Al-MOF (blue curve) (**e**). The UV-Vis spectra of Au NPs (black curve), Apt-Au (red curve), Ru,Al-MOF (blue curve), tracking agent (pink curve) (**f**)
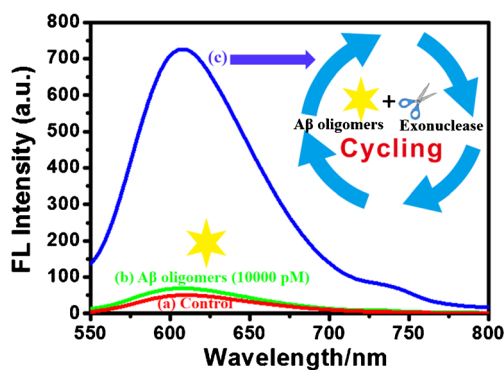
Fig. 2 The fluoresce responses of the tracking agent without Aβ oligomers (a) and after adding 10,000 pM Aβ oligomers (b) 10,000 pM Aβ oligomers and with 200 U·mL^{-1} Rec Jf exonuclease (c). The incubating temperature of all experiments is 37 °C. The wavelength of excitation is 466 nm

Fig. 4 The selectivity of the tracking agent. Error bar: standard deviation for $n = 6$

The tracking agents (aptamer-Au NPs/Ru, Al MOF) were collected by centrifugation for 10 min in the pretreatment and washed with DI water for three times. The obtained conjugates were dispersed into 1.0 mL PBS and stored at 4 °C.

Preparation of aptasensor for Aβ oligomers determination

The manufacturing procedure of the aptasensor for Aβ oligomers is shown in Scheme 1. To detect Aβ oligomers, 200 μL variable concentrations of Aβ oligomers and Rec Jf exonuclease (200 U·mL^{-1}) were added into tracking agent and incubated at room temperature for 30 min. Then the solution was shaken plentifully for quantitative at excited 466 nm by fluorescence spectrophotometer FL-4600. For simplicity of measurement, the experiments were performed at room temperature.

Results and discussion

Characterization of Ru,Al-MOF, aptamer-au NPs, tracking agent

Ru,Al-MOF, aptamer-Au NPs, tracking agent samples were characterized by scanning electron microscope (SEM), transmission electron microscope (TEM) and Brunauer-
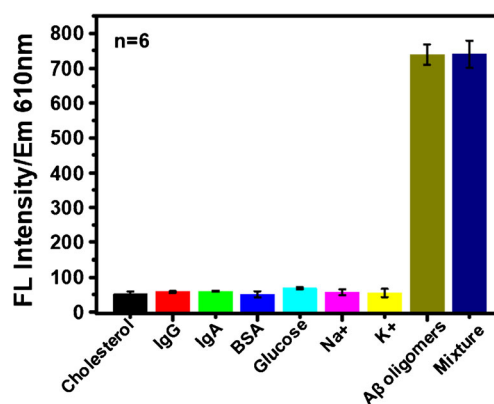
Emmett-Teller (BET), Fourier transform infrared spectroscopy (FTIR), and UV-Vis spectrophotometry. The results are shown in Fig. 1. The SEM image of the Ru,Al-MOF nanospheres depicts the average diameter of 108.6 nm and its rough surface (Fig. 1a). The TEM image of the Ru,Al-MOF nanospheres implies the successful octahedron of Ru,Al-MOF nanospheres in Fig. 1b. In addition, BET surface area for meso Ru,Al-MOF nanospheres (Fig. 1d) and powder XRD the patterns of simulated Ru,Al-MOF nanospheres also prove the successful synthesis and relatively uniform particle size in Fig. S1 and Fig. S2 [28]. The detailed pore size distribution calculated by the BET method suggests that meso Ru,Al-MOF nanospheres have uniform mesoporous size of about 2.2 to 1.3 nm (the detail shown in Fig. 1d). The size of Au nanoparticles had a spherical-shaped morphology observed by transmission electron microscopy (TEM, Fig. S3) with a particle size of 5.214 ± 3.601 nm determined by dynamic light scattering (DLS, $n = 6$ batches). Analysis of size distributions of the tracking agent reveals the average size of 118.9 ± 28.6 nm (the detail shown in Fig. 1c and Fig. S4) and is much larger 10.32 ± 1.25 nm than that of pristine Ru, Al MOF, for which the surface of tracking agent is well covered with a layer of 5 nm Au nanoparticles. The fourier transform infrared spectra of the Ru, Al MOF (Fig. 1e, blue curve) exhibits characteristic peaks at 1037, 1376, 1633 and 2412 cm^{-1} for the

Fig. 3 a The fluorescence responses of tracking agent (turn off, red curve), after adding) 10,000 pM Aβ oligomers and with 200 U·mL^{-1} Rec Jf exonuclease (black curve); **b** The UV-vis absorption spectra of aptamer-Au NPs (black curve), the fluoresce responses of Ru, Al MOF. The wavelength of excitation is 466 nm
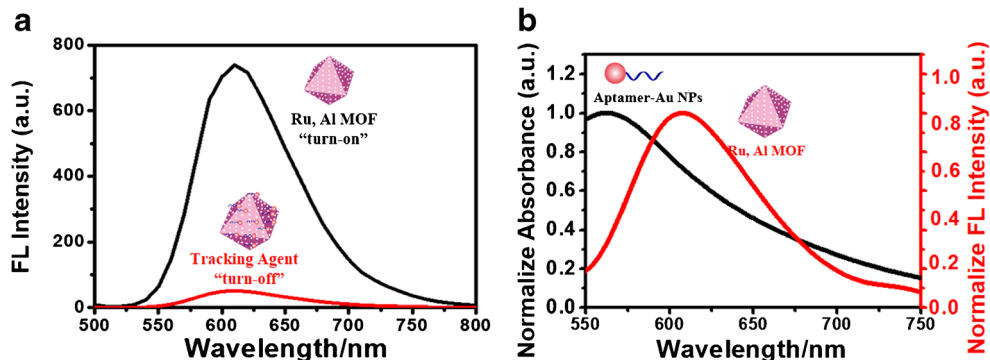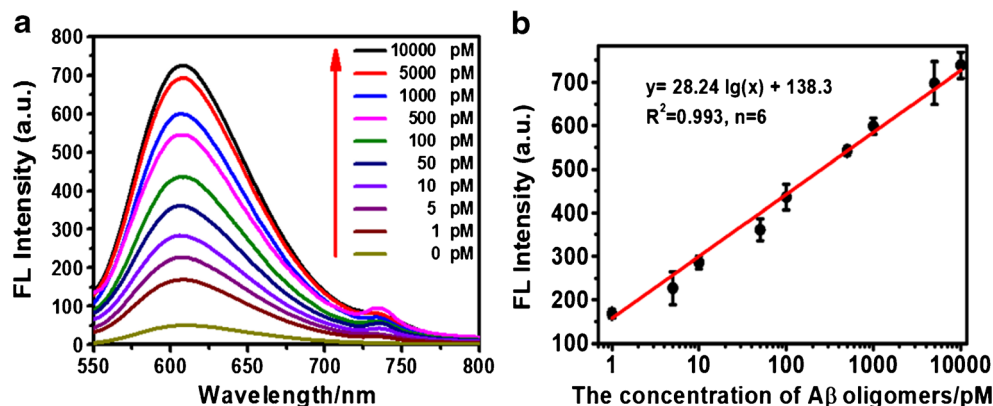
Fig. 5 Fluorescence spectra of the tracking agent in the presence of different concentrations of Aβ oligomers target, (**b**) calibration plot of the proposed fluorescence intensity in the presence of different concentrations of Aβ oligomers target. The wavelength of excitation/emission is 466/610 nm. Error bar: standard deviation for $n = 6$

ring vibrations of bipyridine, peaks at 1608 and 1512 cm^{-1} for the –COO$^-$ asymmetric stretching and peaks at 1435 and 1417 cm^{-1} for –COO$^-$ symmetric stretching. The additional absorption peak at 1669 cm^{-1} is due to the –COOH group of unreacted 2-aminotropephthalic acid molecules trapped in the cavities of Ru, Al MOF [29]. The ultraviolet visible absorption spectra of Au NPs (black curve), Apt-Au NPs (red curve), Ru,Al-MOF (blue curve), tracking agent (pink curve) are shown in Fig. 1f. As shown in black curve and red curve, Apt-Au NPs shows the maximum absorption peak at 266 nm(the characteristic peak of dsDNA) and 552 nm (the Au NPs shifted toward the longer wavelength) [14]. The maximum absorption wavelength of Ru, Al MOF shifts red from 275 nm (the characteristic peak of dsDNA) to 280 nm for the interaction between Apt-Au NPs and Ru,Al-MOF [30].

The signal amplification performance by enzyme-assisted target recycling The fluorescence response of the Ru,Al-MOF was detected to verify the signal amplification efficiency. As shown in Fig. 2, when 10,000 ᴘM Aβ oligomers is added into tracking agent, the fluorescence intensity increases to 18.88 (green curve) compared with no Aβ oligomers added (red curve). While 200 U·mL^{-1} Rec Jf exonuclease and 10,000 ᴘM Aβ oligomers are added, the response significantly increases to 687.73 (blue curve) by about 36.4 folds. All these prove that 200 U·mL^{-1} Rec Jf exonuclease can increase the

Table 1 The different detection methods for Aβ oligomers

Method	Target analyte: Aβ oligomers(pM)		Reference
	Linear range	LOD	
Fluorescence	2000×10^3–$10,000 \times 10^3$	–	[31]
Immunoassay	–	69.8	[32]
SERS	0.1×10^3–$10,000 \times 10^3$	37	[33]
ELISA	20–160	20	[34]
Colorimetric	1–600×10^3	0.56×10^3	[35]
This mothed	1–10,000	0.3	This method

sensitivity, which attributes to the selective digestion of the Aβ oligomers-Apt from 5′ to 3′ by Rec Jf exonuclease in the supernatant solution to release aptamer-Aβ oligomers complex again for analyte recycling.

The detection mechanism of fluorescent aptasensor and increased sensitivity performance The fluorescence spectroscopy of Ru, Al MOF and tracking agent were measured by fluorescence spectrometer to further verify the feasibility of florescence energy transfer (FRET) (the detail shown in Fig. 3a). Upon Ru, Al MOF is bound by Apt-Au NPs to form tracking agent, the strong fluorescence intensity of Ru, Al MOF will "turn-off". Besides, Fig. 3b (black curve) displays that the fluorescence emission of Ru, Al MOF is overlapped with the absorption of Apt-Au NPs large extent. The fluorescence resonance energy transfer between Ru,Al-MOF and Au-Apt NPs is successfully achieved because of this necessary overlap in fluorescence system for efficient energy transfer.

Optimization of experimental condition The reaction time of the tracking agent and Aβ oligomers, the incubation temperature, concentration of tracking agent and Rec Jf exonuclease seriously affected the fluorescence intensity response in Fig. S5. Based on the Fig. S5A, when the time increased from 0 to 50 min, the FL intensity increased considerably from 0 to 719 and then remained almost constant for the long time. The experimental results indicate that the optimal reaction time of the tracking agent and Aβ oligomers is 30 min. The fluorescence signal first increases and then reduces with the increasing of incubation temperature from 20 to 45 °C with a maximum absorbance value at 37 °C in Fig. S5B. Finally, in order to select the most suitable concentration of Rec Jf exonuclease, different concentrations of Rec Jf exonuclease from 50 to 250 U·mL^{-1} was attempted and the maximum fluorescence intensity value is 200 U·mL^{-1} in Fig. S5C.

Selectivity of the Aβ oligomer assay This was tested with Aβ oligomers and major constituents in the blood (cholesterol

Table 2 This method and ELISA method for Aβ oligomers determination ($\overline{x} \pm s$, $n = 5$)

Samples number	Blank (nM)	Added (nM)	Proposed method (nM)	ELISA (nM)	Recovery (%)
1	0	0.1000	0.1010 ± 0.0100	0.1001 ± 0.0120	101.00
	0	1.000	1.020 ± 0.300	1.000 ± 0.051	102.00
2	0	0.1000	0.09301 ± 0.02100	0.09103 ± 0.01806	93.01
	0	1.000	1.012 ± 0.023	0.09801 ± 0.01601	101.20
3	0	0.1000	0.1022 ± 0.0256	0.09306 ± 0.02401	102.20
	0	1.000	1.0184 ± 0.0192	1.012 ± 0.025	101.84

5.0 mM, IgG 10 mg/mL, IgA 6.6 mg/mL, BSA 0.5 mg/mL, glucose 3 mM, K^+ 4 mM, Na^+ 140 mM). These major constituents with identical concentration (10 nM) were respectively added into the incubation liquid. Compared with the interfering samples, the absorbance of target Aβ oligomers is nearly identical with target Aβ oligomers alone due to the specific interaction between the aptamer and the target molecule (in Fig. 4), which demonstrates that these aptamer can only identify Aβ oligomers without interference of major constituents in the blood.

Analytical performance of the fluorometric assay Under the optimal conditions, the sensitivity and detection range of fluorescence assay were tested with a series of concentrations of Aβ oligomers at 610 nm fluorescence emission wavelength. As shown in Fig. 5, the fluorescence increases linearly with the concentration of Aβ oligomers varied from 1.0 pM to 10 nM. The relationship can be described as $y = 28.24\lg(x) + 138.3$ with correlation coefficient of 0.9931, demonstrating a favorable linear relationship. The determination ascribes to the highly fluorescence intensity of Ru, Al MOF as signal and enzyme-exonuclease assisted target recycling to significantly amplify the fluorescence. The reproducibility of the sensor system is appraised by five repeated Aβ oligomers measurement of 10 nM and 1.0 pM. The relative standard deviation (RSD) is about 4.27% and 3.71%, indicating that the proposed method can be employed for the determination of Aβ oligomers with a wide range of concentrations. Determination results of Aβ oligomers with different methods are summarized in Table 1, including fluorescence, immunoassay, surface enhanced raman spectroscopy (SERS), ELISA and colorimetric [31–35]. In this study, the detection limit (LOD) is as low as 0.30 pM and the linear relational concentration range achieves 5 orders of magnitude. The LOD was calculated as the average value of fluorescence intensity at blank concentration of solution at 5 standard deviations (SD).)

Analytical application In order to search the practical application of the tracking agent, the standard addition assay was applied to evaluate the practical applicability of the proposed aptasensor. First, 3 mL healthy human blood serum samples were diluted to 5 mL with PBS (pH 7.4). Then, a collection of samples was done by adding Aβ oligomers with different concentrations to human blood serum. The recoveries are all between 93.01% and 102.20% (Table 2), indicating a good accuracy and applicability of the proposed homogeneous turn-on fluorescent strategy for Aβ oligomers detection.

Conclusion

The homogeneous "turn-on" fluorescent aptasensor detects Aβ oligomers with high selectivity and accuracy based on luminescence MOF nanocomposites as tracking agent and exonuclease-assisted target recycling. The assay has excellent linear response to Aβ oligomers from 1.000 pM to 10,000 pM and detection limit down to 0.3000 pM. The method shows advantage of anti-interference, non-invasion to use and excellent selectivity toward the targets. This system successful applied in real blood sample, which suggests that the platform has great potential for the diagnosis and study of Alzheimer's disease.

References

1. Qin J, Park JS, Jo DG, Cho M, Lee Y (2018) Curcumin-based electrochemical sensor of amyloid-β oligomer for the early detection of Alzheimer's disease. Sensors Actuators B Chem 273:1593–1599. https://doi.org/10.1016/j.snb.2018.07.078
2. Chae MS, Yoo YK, Kim J, Kim TG, Hwang KS (2018) Graphene-based enzyme-modified field-effect transistor biosensor for monitoring drug effects in Alzheimer's disease treatment. Sensors Actuators B Chem 272:448–458. https://doi.org/10.1016/j.snb.2018.06.010

3. Ding S, Cao S, Liu Y, Lian Y, Zhu A, Shi G (2017) Rational design of a stimuli-responsive polymer electrode interface coupled with in vivo microdialysis for measurement of sialic acid in live mouse brain in Alzheimer's disease. ACS Sensors 2(3):394–400. https://doi.org/10.1021/acssensors.6b00772

4. Feng Y, Wang XP, Yang SG, Wang YJ, Zhang X, Du XT, Liu RT (2009) Resveratrol inhibits beta-amyloid oligomeric cytotoxicity but does not prevent oligomer formation. Neurotoxicology 30(6): 986–995. https://doi.org/10.1016/j.neuro.2009.08.013

5. Lee EB, Leng LZ, Zhang B, Kwong L, Trojanowski JQ, Abel T, Lee VMY (2006) Targeting amyloid-β peptide (Aβ) oligomers by passive immunization with a conformation-selective monoclonal antibody improves learning and memory in Aβ precursor protein (APP) transgenic mice. J Biol Chem 281(7):4292–4299. https://doi.org/10.1074/jbc.M511018200

6. Salvadores N, Shahnawaz M, Scarpini E, Tagliavini F, Soto C (2014) Detection of misfolded Aβ oligomers for sensitive biochemical diagnosis of Alzheimer's disease. Cell Rep 7(1):261–268. https://doi.org/10.1016/j.celrep.2014.02.031

7. El-Agnaf OM, Salem SA, Paleologou KE, Curran MD, Gibson MJ, Court JA, Allsop D (2006) Detection of oligomeric forms of α-synuclein protein in human plasma as a potential biomarker for Parkinson's disease. FASEB J 20(3):419–425. https://doi.org/10.1016/j.celrep.2014.02.031

8. Yu Y, Sun X, Tang D, Li C, Zhang L, Nie D, Shi G (2015) Gelsolin bound β-amyloid peptides (1–40/1–42): electrochemical evaluation of levels of soluble peptide associated with Alzheimer's disease. Biosens Bioelectron 68:115–121. https://doi.org/10.1016/j.bios.2014.12.041

9. Jayasena SD (1999) Aptamers: an emerging class of molecules that rival antibodies in diagnostics. Clin Chem 45(9):1628–1650

10. Chen A, Yang S (2015) Replacing antibodies with aptamers in lateral flow immunoassay. Biosens Bioelectron 71:230–242. https://doi.org/10.1016/j.bios.2015.04.041

11. Zhu L, Zhang J, Wang F, Wang Y, Lu L, Feng C, Zhang W (2016) Selective amyloid β oligomer assay based on abasic site-containing molecular beacon and enzyme-free amplification. Biosens Bioelectron 78:206–212. https://doi.org/10.1016/j.bios.2015.11.048

12. Hughes ZE, Walsh TR (2017) Structural disruption of an adenosine-binding DNA aptamer on graphene: implications for Aptasensor design. ACS Sensors 2(11):1602–1611. https://doi.org/10.1021/acssensors.7b00435

13. Liu S, Cheng C, Liu T, Wang L, Gong H, Li F (2015) Highly sensitive fluorescence detection of target DNA by coupling exonuclease-assisted cascade target recycling and DNAzyme amplification. Biosens Bioelectron 63:99–104. https://doi.org/10.1016/j.bios.2014.07.023

14. Miao Y, Gan N, Li T, Cao Y, Hu F, Chen Y (2016) An ultrasensitive fluorescence aptasensor for chloramphenicol based on FRET between quantum dots as donor and the magnetic SiO$_2$@ au NPs probe as acceptor with exonuclease-assisted target recycling. Sensors Actuators B Chem 222:1066–1072. https://doi.org/10.1016/j.snb.2015.09.049

15. Huang YL, Gao ZF, Luo HQ, Li NB (2017) Sensitive detection of HIV gene by coupling exonuclease III-assisted target recycling and guanine nanowire amplification. Sensors Actuators B Chem 238: 1017–1023. https://doi.org/10.1016/j.snb.2016.07.144

16. Pham TT, Yin J, Eid JS, Adams E, Lam R, Turner SW, Hanes JW (2016) Single-locus enrichment without amplification for sequencing and direct detection of epigenetic modifications. Mol Gen Genomics 291(3):1491–1504. https://doi.org/10.1007/s00438-016-1167-2

17. Chen M, Gan N, Zhou Y, Li T, Xu Q, Cao Y, Chen Y (2016) An electrochemical aptasensor for multiplex antibiotics detection based on metal ions doped nanoscale MOFs as signal tracers and RecJf exonuclease-assisted targets recycling amplification. Talanta 161: 867–874. https://doi.org/10.1016/j.talanta.2016.09.051

18. Zhu X, Su Q, Feng W, Li F (2017) Anti-stokes shift luminescent materials for bio-applications. Chem Soc Rev 46(4):1025–1039. https://doi.org/10.1039/C6CS00415F

19. Fan C, Lv X, Liu F, Feng L, Liu M, Cai Y, Wang H (2018) Silver nanoclusters encapsulated into metal–organic frameworks with enhanced fluorescence and specific ion accumulation toward the microdot array-based fluorimetric analysis of copper in blood. ACS Sensors 3(2):441–450. https://doi.org/10.1021/acssensors.7b00874

20. Zhang Y, Yuan S, Day G, Wang X, Yang X, Zhou HC (2018) Luminescent sensors based on metal-organic frameworks. Coord Chem Rev 354:28–45. https://doi.org/10.1016/j.ccr.2017.06.007

21. Zhang L, Kang Z, Xin X, Sun D (2016) Metal–organic frameworks based luminescent materials for nitroaromatics sensing. CrystEngComm 18(2):193–206. https://doi.org/10.1039/C5CE01917F

22. Chen S, Shi Z, Qin L, Jia H, Zheng H (2016) Two new luminescent cd (II)-metal–organic frameworks as bifunctional chemosensors for detection of cations Fe^{3+}, anions CrO$_4^{2-}$, and Cr$_2$O$_7^{2-}$ in aqueous solution. Cryst Growth Des 17(1):67–72. https://doi.org/10.1021/acs.cgd.6b01197

23. Lian X, Fang Y, Joseph E, Wang Q, Li J, Banerjee S, Zhou HC (2017) Enzyme–MOF (metal–organic framework) composites. Chem Soc Rev 46(11):3386–3401. https://doi.org/10.1039/C7CS00058H

24. Fang JM, Leng F, Zhao XJ, Hu XL, Li YF (2014) Metal–organic framework MIL-101 as a low background signal platform for label-free DNA detection. Analyst 139(4):801–806. https://doi.org/10.1039/C3AN01975F

25. Maza WA, Haring AJ, Ahrenholtz SR, Epley CC, Lin SY, Morris AJ (2016) Ruthenium (II)-polypyridyl zirconium (IV) metal–organic frameworks as a new class of sensitized solar cells. Chem Sci 7(1):719–727. https://doi.org/10.1039/C5SC01565K

26. Radenković S, Antić M, Savić ND, Glišić BĐ (2017) The nature of the au–N bond in gold (iii) complexes with aromatic nitrogen-containing heterocycles: the influence of au (iii) ions on the ligand aromaticity. New J Chem 41(21):12407–12415. https://doi.org/10.1039/C7NJ02634J

27. Yin HQ, Yang JC, Yin XB (2017) Ratiometric fluorescence sensing and real-time detection of water in organic solvents with one-pot synthesis of Ru@ MIL-101 (Al)–NH$_2$. Anal Chem 89(24):13434–13440. https://doi.org/10.1021/acs.analchem.7b03723

28. Chołuj A, Zieliński A, Grela K, Chmielewski MJ (2016) Metathesis@ MOF: simple and robust immobilization of olefin metathesis catalysts inside (Al) MIL-101-NH$_2$. ACS Catal 6(10): 6343–6349. https://doi.org/10.1021/acscatal.6b01048

29. El-Mehalmey WA, Ibrahim AH, Abugable AA, Hassan MH, Haikal RR, Karakalos SG, Alkordi MH (2018) Metal–organic framework@ silica as a stationary phase sorbent for rapid and cost-effective removal of hexavalent chromium. J Mater Chem A 6(6):2742–2751. https://doi.org/10.1039/C7TA08281A

30. Lapitan LD Jr, Guo Y, Zhou D (2015) Nano-enabled bioanalytical approaches to ultrasensitive detection of low abundance single nucleotide polymorphisms. Analyst 140(12):3872–3887. https://doi.org/10.1039/C4AN02304H

31. Lv G, Sun A, Wei P, Zhang N, Lan H, Yi T (2016) A spiropyran-based fluorescent probe for the specific detection of β-amyloid peptide oligomers in Alzheimer's disease. Chem Commun 52(57):8865–8868. https://doi.org/10.1039/C6CC02741E

32. Park MC, Kim M, Lim GT, Kang SM, An SSA, Kim TS, Kang JY (2016) Droplet-based magnetic bead immunoassay using microchannel-connected multiwell plates (μCHAMPs) for the detection of amyloid beta oligomers. Lab Chip 16(12):2245–2253. https://doi.org/10.1039/C6LC00013D

33. Zhang X, Liu S, Song X, Wang H, Wang J, Wang Y, Huang J, Yu J (2019) Robust and universal SERS sensing platform for multiplexed detection of Alzheimer's disease Core biomarkers using PAapt-AuNPs conjugates. ACS Sensors 4(8):2140–2149. https://doi.org/10.1021/acssensors.9b00974

34. Zhou J, Meng L, Ye W, Wang Q, Geng S, Sun C (2018) A sensitive detection assay based on signal amplification technology for Alzheimer's disease's early biomarker in exosome. Anal Chim Acta 1022(31):124–130. https://doi.org/10.1016/j.aca.2018.03.016

35. Zhu X, Zhang N, Zhang Y, Liu B, Chang Z, Zhou Y, Xu M (2018) A sensitive gold nanoparticle-based aptasensor for colorimetric detection of Aβ 1–40 oligomers. Anal Methods 10(6):641–645. https://doi.org/10.1039/C7AY02918G